Research Article | Vol. 7, No. 12 | 1 Dec 2016 | BIOMEDICAL OPTICS EXPRESS 5042

Biomedical Optics EXPRESS

Spectrometer calibration for spectroscopic Fourier domain optical coherence tomography

MACIEJ SZKULMOWSKI,* SZYMON TAMBORSKI, AND MACIEJ WOJTKOWSKI

Institute of Physics, Faculty of Physics, Astronomy and Informatics, Nicolaus Copernicus University, Grudziadzka 5, 87-100 Torun, Poland
maciej.szkulmowski@fizyka.umk.pl

Abstract: We propose a simple and robust procedure for Fourier domain optical coherence tomography (FdOCT) that allows us to linearize the detected FdOCT spectra to a wavenumber domain and, at the same time, determine the wavelength of light for each point of the detected spectrum. We show that in this approach it is possible to use any measurable physical quantity that has linear dependency on wavenumber and can be extracted from spectral fringes. The actual values of the measured quantity have no importance for the algorithm and do not need to be known at any stage of the procedure. As an example, we calibrate a spectral OCT spectrometer using Doppler frequency. The technique of spectral calibration can be in principle adapted to of all kind of Fourier domain OCT devices.

OCIS codes: (110.2970) Image detection systems; (110.4500) Optical coherence tomography; (300.0300) Spectroscopy; (300.6170) Spectra; (300.6190) Spectrometers.

References and links

1. A. F. Fercher, C. K. Hitzenberger, G. Kamp, and S. Y. Elzaiat, "Measurement of Intraocular Distances by Backscattering Spectral Interferometry," Opt. Commun. **117**(1-2), 43–48 (1995).
2. M. Wojtkowski, "High-speed optical coherence tomography: basics and applications," Appl. Opt. **49**(16), D30–D61 (2010).
3. B. Potsaid, I. Gorczynska, V. J. Srinivasan, Y. Chen, J. Jiang, A. Cable, and J. G. Fujimoto, "Ultrahigh speed spectral / Fourier domain OCT ophthalmic imaging at 70,000 to 312,500 axial scans per second," Opt. Express **16**(19), 15149–15169 (2008).
4. T. Klein, W. Wieser, R. Andre, T. Pfeiffer, C. M. Eigenwillig, and R. Huber, "Multi-MHz FDML OCT: Snapshot retinal imaging at 6.7 million axial-scans per second," Optical Coherence Tomography and Coherence Domain Optical Methods in Biomedicine Xvi 8213 (2012).
5. A. Szkulmowska, M. Szkulmowski, D. Szlag, A. Kowalczyk, and M. Wojtkowski, "Three-dimensional quantitative imaging of retinal and choroidal blood flow velocity using joint Spectral and Time domain Optical Coherence Tomography," Opt. Express **17**(13), 10584–10598 (2009).
6. F. Jaillon, S. Makita, and Y. Yasuno, "Variable velocity range imaging of the choroid with dual-beam optical coherence angiography," Opt. Express **20**(1), 385–396 (2012).
7. R. K. K. Wang, "Optical Microangiography: A Label Free 3D Imaging Technology to Visualize and Quantify Blood Circulations within Tissue Beds in vivo," IEEE J. Sel. Top. Quantum Electron. **16**(3), 545–554 (2010).
8. V. Doblhoff-Dier, L. Schmetterer, W. Vilser, G. Garhöfer, M. Gröschl, R. A. Leitgeb, and R. M. Werkmeister, "Measurement of the total retinal blood flow using dual beam Fourier-domain Doppler optical coherence tomography with orthogonal detection planes," Biomed. Opt. Express **5**(2), 630–642 (2014).
9. R. Leitgeb, M. Wojtkowski, A. Kowalczyk, C. K. Hitzenberger, M. Sticker, and A. F. Fercher, "Spectral measurement of absorption by spectroscopic frequency-domain optical coherence tomography," Opt. Lett. **25**(11), 820–822 (2000).
10. D. J. Faber, E. G. Mik, M. C. Aalders, and T. G. van Leeuwen, "Toward assessment of blood oxygen saturation by spectroscopic optical coherence tomography," Opt. Lett. **30**(9), 1015–1017 (2005).
11. F. E. Robles, C. Wilson, G. Grant, and A. Wax, "Molecular imaging true-colour spectroscopic optical coherence tomography," Nat. Photonics **5**(12), 744–747 (2011).
12. B. F. Kennedy, M. Wojtkowski, M. Szkulmowski, K. M. Kennedy, K. Karnowski, and D. D. Sampson, "Improved measurement of vibration amplitude in dynamic optical coherence elastography," Biomed. Opt. Express **3**(12), 3138–3152 (2012).
13. Z. Hu and A. M. Rollins, "Fourier domain optical coherence tomography with a linear-in-wavenumber spectrometer," Opt. Lett. **32**(24), 3525–3527 (2007).
14. V. M. Gelikonov, G. V. Gelikonov, and P. A. Shilyagin, "Linear-wavenumber spectrometer for high-speed spectral-domain optical coherence tomography," Opt. Spectrosc. **106**(3), 459–465 (2009).

#269242 http://dx.doi.org/10.1364/BOE.7.005042
Journal © 2016 Received 5 Jul 2016; revised 15 Oct 2016; accepted 22 Oct 2016; published 9 Nov 2016

Biomedical Optics EXPRESS

15. T. Bajraszewski, M. Wojtkowski, M. Szkulmowski, A. Szkulmowska, R. Huber, and A. Kowalczyk, "Improved spectral optical coherence tomography using optical frequency comb," Opt. Express **16**(6), 4163–4176 (2008).
16. M. A. Choma, K. Hsu, and J. A. Izatt, "Swept source optical coherence tomography using an all-fiber 1300-nm ring laser source," J. Biomed. Opt. **10**(4), 044009 (2005).
17. C. M. Eigenwillig, B. R. Biedermann, G. Palte, and R. Huber, "K-space linear Fourier domain mode locked laser and applications for optical coherence tomography," Opt. Express **16**(12), 8916–8937 (2008).
18. S. Vergnole, D. Lévesque, and G. Lamouche, "Experimental validation of an optimized signal processing method to handle non-linearity in swept-source optical coherence tomography," Opt. Express **18**(10), 10446–10461 (2010).
19. K. Wang and Z. H. Ding, "Spectral calibration in spectral domain optical coherence tomography," Chin. Opt. Lett. **6**(12), 902–904 (2008).
20. S. Makita, T. Fabritius, and Y. Yasuno, "Full-range, high-speed, high-resolution 1 microm spectral-domain optical coherence tomography using BM-scan for volumetric imaging of the human posterior eye," Opt. Express **16**(12), 8406–8420 (2008).
21. D. J. Faber and T. G. van Leeuwen, "Doppler calibration method for Spectral Domain OCT spectrometers," J. Biophotonics **2**(6-7), 407–415 (2009).
22. D. Piao, L. L. Otis, and Q. Zhu, "Doppler angle and flow velocity mapping by combined Doppler shift and Doppler bandwidth measurements in optical Doppler tomography," Opt. Lett. **28**(13), 1120–1122 (2003).
23. S. G. Proskurin, Y. He, and R. K. Wang, "Determination of flow velocity and spectrum broadening with vector based on Doppler shift optical coherence tomography," Opt. Lett. **28**, 1227–1229 (2003).
24. A. Bouwens, D. Szlag, M. Szkulmowski, T. Bolmont, M. Wojtkowski, and T. Lasser, "Quantitative lateral and axial flow imaging with optical coherence microscopy and tomography," Opt. Express **21**(15), 17711–17729 (2013).
25. B. Park, M. C. Pierce, B. Cense, S. H. Yun, M. Mujat, G. Tearney, B. Bouma, and J. de Boer, "Real-time fiber-based multi-functional spectral-domain optical coherence tomography at 1.3 microm," Opt. Express **13**(11), 3931–3944 (2005).
26. M. Szkulmowski, A. Wojtkowski, T. Bajraszewski, I. Gorczynska, P. Targowski, W. Wasilewski, A. Kowalczyk, and C. Radzewicz, "Quality improvement for high resolution in vivo images by spectral domain optical coherence tomography with supercontinuum source," Opt. Commun. **246**(4-6), 569–578 (2005).
27. M. Mujat, B. H. Park, B. Cense, T. C. Chen, and J. F. de Boer, "Autocalibration of spectral-domain optical coherence tomography spectrometers for in vivo quantitative retinal nerve fiber layer birefringence determination," J. Biomed. Opt. **12**(4), 041205 (2007).
28. X. L. Zhang, W. R. Gao, H. Y. Bian, C. L. Chen, and J. L. Liao, "Self-spectral calibration for spectral domain optical coherence tomography," Opt. Eng. **52**, 063603 (2013).
29. T. J. Eom, Y. C. Ahn, C. S. Kim, and Z. Chen, "Calibration and characterization protocol for spectral-domain optical coherence tomography using fiber Bragg gratings," J. Biomed. Opt. **16**(3), 030501 (2011).
30. A. K. Gaigalas, L. Wang, H. J. He, and P. DeRose, "Procedures for Wavelength Calibration and Spectral Response Correction of CCD Array Spectrometers," J. Res. Natl. Inst. Stand. Technol. **114**(4), 215–228 (2009).
31. C. Ding, P. Bu, X. Z. Wang, and O. Sasaki, "A new spectral calibration method for Fourier domain optical coherence tomography," Optik (Stuttg.) **121**(11), 965–970 (2010).
32. J. H. Kim, J. H. Han, and J. Jeong, "Accurate Wavelength Calibration Method for Spectrometer Using Low Coherence Interferometry," J. Lightwave Technol. **33**(16), 3413–3418 (2015).
33. J. H. Kim, J. H. Han, and J. Jeong, "Wavelength calibration of dispersive near-infrared spectrometer using relative k-space distribution with low coherence interferometer," Opt. Commun. **367**, 186–191 (2016).
34. M. Gora, K. Karnowski, M. Szkulmowski, B. J. Kaluzny, R. Huber, A. Kowalczyk, and M. Wojtkowski, "Ultra high-speed swept source OCT imaging of the anterior segment of human eye at 200 kHz with adjustable imaging range," Opt. Express **17**(17), 14880–14894 (2009).
35. M. Szkulmowski, S. Tamborski, and M. Wojtkowski, "Wavelength to pixel calibration for FdOCT," Optical Coherence Tomography and Coherence Domain Optical Methods in Biomedicine Xix 9312 (2015).
36. M. Szkulmowski, A. Szkulmowska, T. Bajraszewski, A. Kowalczyk, and M. Wojtkowski, "Flow velocity estimation using joint Spectral and Time domain Optical Coherence Tomography," Opt. Express **16**(9), 6008–6025 (2008).
37. M. Szkulmowski, I. Grulkowski, D. Szlag, A. Szkulmowska, A. Kowalczyk, and M. Wojtkowski, "Flow velocity estimation by complex ambiguity free joint Spectral and Time domain Optical Coherence Tomography," Opt. Express **17**(16), 14281–14297 (2009).
38. M. Szkulmowski and M. Wojtkowski, "Averaging techniques for OCT imaging," Opt. Express **21**(8), 9757–9773 (2013).

1. Introduction

Fourier domain Optical Coherence Tomography (FdOCT) [1] is a well-established imaging technique with micrometer resolution and high sensitivity [2]. State of the art devices allow for acquisition hundred thousand or millions light spectra per second in most common modalities of the technique: Spectral OCT (SOCT) [3] and Swept Source OCT (SSOCT) [4].

Biomedical Optics EXPRESS

Due to the high acquisition speeds and high resolution it is not only used to morphological imaging but also to functional studies, such as blood velocity estimation [5–8], assessment of spectroscopic [9–11] or elastic properties of samples [12].

In order to achieve highest possible performance of the FdOCT systems it is necessary to have the registered spectra linearized in wavenumbers. This allows to maximize the axial resolution and sensitivity as well as minimize the sensitivity roll-off. The linearization of registered spectra in wavenumber domain is possible in two ways, either by acquisition of the spectra uniformly sampled in wavenumbers or by numerical linearization of the data registered in a measurement space. The former can be achieved in SOCT by use of linear-k spectrometers [13, 14] or light spectrum filtered with Fabry-Perot filters [15] and in SSOCT by use of external k-clocks [16] or tailored laser sources [17]. In most cases however, the spectra are not registered linearly in wavenumbers so prior to further processing have to be numerically linearized. A lot of effort has been put into construction of effective mapping algorithms [18]. The most common way of accurate mapping of function from the acquisition space to wavenumber space is to use phase of Hilbert transformed spectrum acquired with a mirror as a sample. In case no dispersion mismatch between the arms of the FdOCT interferometer is present, the phase of such fringes is linear in wavenumber so a mapping function can easily be found. A modification of this technique requires two measurements of a mirror placed in two different depth positions and allows to obtain dispersion free modulation of spectral fringes [19, 20], what greatly simplifies the adjusting procedure since dispersion mismatch is hard to be removed completely in real life interferometers. In principle, the linearization can be performed using any measurable quantity known to have linear dependency on wavenumbers. For example, the phase of the harmonically modulated light spectrum filtered by a Fabry-Perot filter has been used or frequency of the Doppler signal introduced by a moving mirror [21].

More accurate calibration is required in case of functional studies. Knowledge about wavelength of measured spectral fringes, although not necessary for reconstruction of structural images, is favorable in Doppler OCT and essential in spectroscopic OCT. In Doppler OCT calculations of axial velocity values require mean wavelength of used light source and determination of value of transverse velocity requires additionally spectral spread [22–24]. Now, to calibrate Doppler OCT the required values are taken from light source specifications, but this gives only approximate results since the effective light spectrum parameters change during propagation through optical elements of the setup and the sample. In spectroscopic OCT the requirement of exact mapping of wavelength to the registered spectral points is self-explanatory.

Existing techniques of mapping wavenumbers to points of registered spectra are based on various concepts. Spatial distribution of wavelengths on the detector points can be calculated directly from the spectrometer geometry [25, 26]. Although this approach has limited accuracy, it can be improved with the use of either an iterative correction techniques [27, 28] or narrow spectral lines from fiber Bragg gratings [29] and krypton lamp [30]. Comparison of spectra registered by a calibrated spectrum analyzer and by the spectrometer to be calibrated has been shown by Ding *et al.* [31]. Recently, additional light sources with narrow spectral lines from argon lamp have been used to assign wavenumbers to pixels in SOCT spectrometers by Kim *et al*. [32, 33]. In these two steps approaches zero-crossing detection is applied to single component spectral fringe signal to extract the distribution of spectrometer points equidistant in wavenumber space. This step is followed by calculation of absolute wavenumbers for all points of the detector using information provided either by calibration lamp with multiple spectral lines [33] or by recalculation of spectral range of the spectrometer from imaging range of the SOCT device [32]. Another interesting approach was presented by Faber *et al.* [21] where the Doppler frequency was introduced in data acquired during motion of a mirror used as a sample. Since the Doppler frequency for each pixel is a product of mirror velocity and wavenumber, it can be used to both spectrometer linearization and mapping

Biomedical Optics EXPRESS

wavenumbers to points of registered spectra. The precision of the mapping depends in this technique on the exact knowledge of the mirror velocity.

Among the aforementioned techniques the use of calibration lamps may seem to be the most straightforward way to calibrate a spectrometer, Although this approach is conceptually simple and provides sufficient precision, it has not become common in FdOCT community. Several reasons may be the cause of such situation. First of all, the necessity to use additional light source for calibration increases the overall cost and complexity of experimental setups, but most importantly, to provide good calibration accuracy such source should evenly cover the spectral range of the spectrometer with narrow spectral lines. As the fast development of imaging techniques based on FdOCT opens to new spectral ranges and new configurations of devices this requirement may be hard to achieve for a single source. Because difficulties in access to necessary calibration source could hinder the development of new devices, new techniques that use only data acquired with the FdOCT setup to be calibrated are desirable.

In this work we propose a method that has all the desired features for comprehensive spectral calibration technique for Fourier domain OCT spectra, It comprises linearization of spectra to wavenumber domain, removal of uncompensated dispersion and assignment of wavenumber to each point of the spectrum. The technique can use any physical quantity known to have linear dependence on wavenumber that can be derived from data measured by the FdOCT setup. The main difference between our approach and the previously reported ones is that here the actual values of this quantity do not need to be known, but can be also calculated during the process of calibration, what makes it particularly robust. The only parameter of the SOCT system that has to be precisely found is the depth imaging range, which can be easily and with high precision measured in a simple single additional experiment.

As example we calibrated a SOCT spectrometer equipped with a mirror in the sample arm of the interferometer (which is a standard approach during any SOCT setup characterization procedures). As the physical quantity we used Doppler frequency induced in each point of the detected spectrum by a motion of the sample arm mirror. To validate the results a set of spectral lines emitted by optical parametric oscillator was simultaneously registered by an optical spectrum analyzer and by the SOCT spectrometer calibrated with our technique.

2. Theory

The calibration procedure consists of two major steps. In the first step, the acquired SOCT spectra need to be linearized to provide equal distance between points in wavenumber domain. In the second step wavenumber is assigned to each point of the linearized spectrum. In principle, in both steps the same data set can be used since both steps require a physical quantity known to have linear dependence on wavenumber. But this is not a strict requirement and in practical solutions it may sometimes be useful to use different data at every step.

2.1. Linearization of FdOCT spectra in wavenumber domain

In a general case in the FdOCT setup, a single acquired interferometric signal is nonlinear due to two independent factors: nonlinear sampling of the spectra and uncompensated dispersion mismatch between the arms of the interferometer. Usual procedure of linearization of the signal is composed of two steps: resampling the spectra to wavenumber space followed by multiplication of the result by a complex vector to remove the impact of dispersion mismatch. The two components are independent and each of them can easily be found when the other effect is absent in the registered signal.

In the first step the phase is corrected for nonlinear sampling. In this step any physical quantity that is linearly depended on wavenumber and is possible to be detected with the spectrometer can be used. Having the values of the physical quantity q registered for each point of the spectrum our approach presented by Gora et al. [34] can be applied to find the fractional values of points of the spectrum with equidistant wavenumbers. In brief, a

Biomedical Optics EXPRESS

polynomial of a rank r is fit to find a relation between a number of spectral point n_k and the physical quantity $n_k = P_k^{(r)}(q)$. Next, the values of q are found, for which the polynomial takes values of the number of the first and the last point of the spectrum: $P_k^{(r)}(q_{first}) = 0$ and $P_k^{(r)}(q_{last}) = N_k - 1$, where N_k is the number of points in the spectrum. Fractional values of points for which the spectrum is equally spaced in wavenumbers (that for simplicity we call "resampling indexes") may be calculated simply by:

$$n_i = P_k^{(r)}\left(q_{first} + i \cdot \frac{q_{last} - q_{first}}{N_k - 1}\right), \tag{1}$$

where $i = 0, \ldots, N_k - 1$. The final step is resampling the spectra to obtain its values for the resampling indexes.

The simplest quantity q that can be measured is the unwrapped phase of the registered spectral fringes acquired with a mirror as an object. Unfortunately, this phase is not only dependent on the optical path difference between the arms of the interferometer but also by the dispersion mismatch. Therefore, the impact of dispersion on the spectral fringes phase has to be removed. The straightforward approach is a careful hardware dispersion matching using blocks of glass inserted in the arms of the interferometer, but usually it is not sufficient to completely remove it. In 2008 to solve this problem Makita [20] and Wang [19] proposed to use the difference of phases calculated from two spectra acquired for two optical path differences. Such a phase difference does not depend on dispersion mismatch and allows to calculate the mapping function for linearization of the spectrometer.

Another possible quantity q is the Doppler frequency that appears in spectral fringes registered in time with constant motion of one of the mirrors in the experimental setup. This approach has been first used by Faber and al. in 2009 [21]. Since the Doppler frequency does not depend on the uncompensated dispersion it can be used directly as without any additional preprocessing.

Regardless the used quantity q an important problem is to find a proper rank $_r$ of the polynomial in Eq. (1). During this study we found that the rank need to be optimized, but even a trivial search procedure is effective enough and fast. For a chosen q we generate resampling indexes for different ranks of the polynomial. As optimal we choose the resampling indexes that lead to minimal resolution drop along z-axis.

In the second step of fringe phase linearization, after canceling the effect of nonlinear sampling, the impact of dispersion mismatch can be calculated and compensated. From a resampled spectra with only one frequency component, for example from a simple mirror, the unwrapped phase is extracted:

$$\Phi(k) = 2zk + \phi_D(k). \tag{2}$$

In this phase, it is assumed that the only source of nonlinearity is the uncompensated dispersion mismatch $\phi_D(k)$. In order to find the nonlinear component from the fringes we fit the calculated phase with a line, which we subtract from phase described by Eq. (2):

$$\phi_D(k) \cong \Phi(k) - linear.fit(\Phi(k)). \tag{3}$$

This phase difference is used to create complex valued dispersion corrector $\exp(-i\phi_D(k))$ which is multiplied with the previously resampled spectrum. As a final step a spectral shaping can be performed to reduce sidelobes in the point spread function of the system [26].

Biomedical Optics EXPRESS

2.2. Linearization of FdOCT spectrum in time domain

Apart of the phase linearization in the wavenumber domain a similar linearization may also be needed to be performed in the time domain. Spectral data with frequency in time domain are gathered for example for purposes of spectrometer calibration in the method proposed by Faber et al. [21] and in the wavelength mapping procedure described in Section 2.4 below that bases on the Spectral and Time domain analysis. Although the sampling in time is equidistant, a nonlinearity in phase of spectral fringes along time may appear, caused by non-constant velocity of the mirror. Therefore, we apply the same procedure of spectrum resampling as for canceling the nonlinear sampling in wavenumber domain. To calculate the points for resampling it is sufficient to use directly the phase of time-dependent modulation caused by the moving mirror, since no time-dependent dispersion effect is present in the configuration. We take the unwrapped phase of time-dependent signal for one point of each spectra and perform similar procedure that led to Eq. (1). Next, we perform resampling along time axis for each wavenumber using the same resampling indexes. It has to be noted that since the resampling procedure preserves all the points of the resampled spectrum, the mean frequency before and after the procedure remains the same.

2.3. Mapping wavelength to spectrum points – general case

In a general case one needs to measure with the spectrometer to be calibrated any physical quantity q that linearly depends on wavenumber. It has to be noted, that in principle it may be the same quantity or even the same measurement that is used to linearize the spectra to wavenumber domain as shown in the previous subsections.

As shown by Szkulmowski *et al.* in [35] after linearization of the spectra fringes to wavenumber domain the value of the quantity q is extracted from i-th point of the spectrum and written as (see also Fig. 1(b)):

$$q_i = \gamma_q \cdot k_i, \tag{4}$$

where, in general, neither factor γ_q nor wavenumbers k_i are known. The parameter γ_q can be expressed as ratio of the total spread ΔQ of the measured quantity q to the total spectral range of the spectrometer ΔK in wavenumber domain:

$$\gamma_q = \frac{\Delta Q}{\Delta K}. \tag{5}$$

The value of $\Delta Q = q_{\max} - q_{\min}$ is taken from experiment, but the ΔK is an unknown parameter, that we express using the imaging range of the FdOCT device $z_{\max}$ [32, 35]:

$$z_{\max} = \frac{\pi}{2\Delta k}, \tag{6}$$

where $\Delta k = \Delta K / N_k$ is spectral spread per one point of the spectrum and N_k is the number of spectral points. Substituting Eq. (6) to Eq. (5) leads to expression for γ_q that depends only on measurable quantities:

$$\gamma_q = \Delta Q \cdot \frac{2 z_{\max}}{\pi N_k}. \tag{7}$$

Now, the relation for wavenumber of the i-th spectrum point can be obtained by substituting Eq. (7) to Eq. (4) and rearranging:

Biomedical Optics EXPRESS

$$k_i = \frac{q_i}{\Delta Q} \cdot \frac{\pi N_k}{2 z_{\max}}, \tag{8}$$

and immediately we obtain also the expression for wavelength for *i*-th point of spectrum:

$$\lambda_i = \frac{\Delta Q}{q_i} \cdot \frac{4 z_{\max}}{N_k}. \tag{9}$$

Important property of expressions given by Eq. (8) and Eq. (9) is that the ratio $\Delta Q / q_i$ is dimensionless. Therefore, the actual values of the measured physical quantity q are not important. For example, if q is detected as a discrete quantity, $\Delta Q / q_i$ can be calculated using simply indexes of points with no scaling. This property will be used in the following Section 2.4 where we will calibrate a spectrometer using Doppler frequencies induced by a moving mirror and use for calculations numbers of DFT points in the signal instead of actual Doppler frequencies.

2.4. Mapping wavelength to spectrum points – Doppler frequency as a mapping function

Let us imagine a simple experiment performed with Spectral OCT system where a single mirror moving with constant velocity v serves as sample. In such case the information carrying component of the detected spectral fringes can be written as follows:

$$I(k,t) \cong \cos\left(2(z+vt)k\right) = \cos\left(2z \cdot k + 2vk \cdot t\right), \tag{10}$$

where z is the initial position of the mirror with respect to the zero optical delay position, k is wavenumber and t stands for time. We can see that a time dependent frequency of fringes can serve as quantity q. Let us therefore define:

$$q_\omega = \gamma_\omega \cdot k \equiv \omega_D = 2v \cdot k. \tag{11}$$

The so called Doppler frequency ω_D can easily be estimated by means of Fourier transformation applied to the time-dependent signal registered for each spectral point. Since Fourier transformation will also be used along wavenumber axis to retrieve phase of the fringes later in the article, it is convenient for us to explain the proposed method using calculation scheme of joint Spectral and Time domain OCT (STdOCT). The technique was introduced in 2008 for axial velocity estimation [36], and afterwards applied to complex ambiguity removal [37], vibration amplitude estimation [12], total flow calculations [24] and increasing image quality of morphological tomograms [38].

The STdOCT calculation scheme uses only Fourier transformations applied in both wavenumber and time directions. The possible transformations can be visualized on the STdOCT diagram as depicted in Fig. 1(a). Fourier transformation applied to each spectrum form kt plane along wavenumber axis transforms data to the depth space (zt plane), where time-dependent information on the position of the mirror $\delta\left(z' - (z+vt)\right)$ can be extracted for each time moment. This is a standard procedure in any SOCT processing schemes. Fourier transformation applied to the data from kt plane along time axis transforms it to the kω plane, where information on the wavelength-dependent Doppler frequency is visible $\delta(\omega' - vk)$. Two consecutive Fourier transformations lead to zω plane, where simultaneously information about position and Doppler frequency can be extracted. In this work, to map wavelength to the points of detected spectra, only information extracted from zt plane and kω plane will be used, and parameters used in the calculations are presented in Fig. 1.

Biomedical Optics EXPRESS

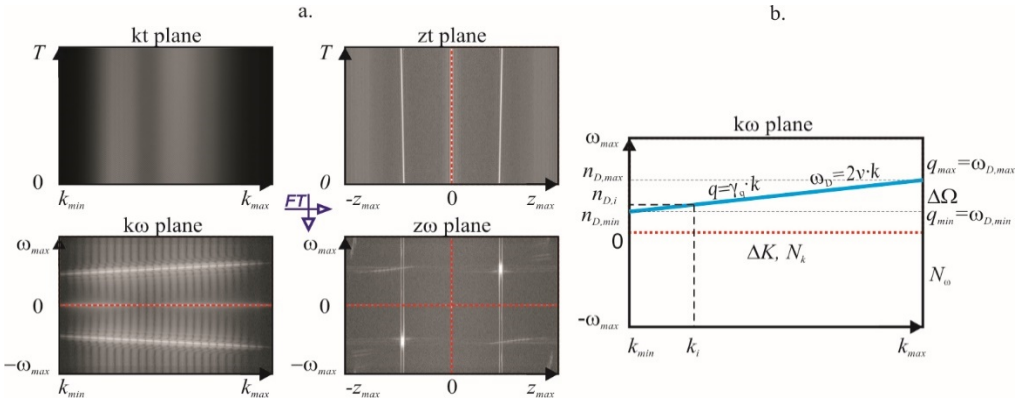

Fig. 1. Parameters used in spectrometer mapping using Doppler frequency. a. STdOCT diagram. Presented data are obtained from the moving mirror experiment. Red dotted lines mark the zero optical delay (vertical) and zero velocity delay (horizontal). Data plotted in all panels are the real valued amplitudes of spectra (kt plane) or its Fourier transforms (other planes). b. kω panel of the STdOCT diagram with the detected Doppler frequency marked as a blue line. $n_{D,min}$ and $n_{D,min}$ are minimal and maximal Doppler frequencies detected from the spectra; $\Delta\Omega = \omega_{D,max} - \omega_{D,min}$ is the Doppler frequency spread; $n_{D,min}$ and $n_{D,max}$ are positions of $\omega_{D,min}$ and $\omega_{D,min}$ in units of Fourier transform points; $n_{D,i}$ is the position of Doppler frequency value of *i*-th spectrum point in units of Fourier transform points; k_i – value of k for *i* -th spectrum point; $\Delta K = k_{max} - k_{min}$ – spectral spread of the spectrometer; N_k – number of points in spectrum; N_ω – number of points in Doppler frequency axis.

By analogy to Eq. (8) using Eq. (11) we can write:

$$k_i = \frac{\omega_{D,i}}{\Delta\Omega} \cdot \frac{\pi N_k}{2z_{\max}}, \tag{12}$$

where $\omega_{D,i}$ is Doppler frequency for *i* -th point of the spectrum and $\Delta\Omega$ is the Doppler frequency spread over all the spectral range registered by the spectrometer. As previously, also the relation for wavelength can be obtained:

$$\lambda_i = \frac{\Delta\Omega}{\omega_{D,i}} \cdot \frac{4z_{\max}}{N_k}. \tag{13}$$

It has to be noted that the Doppler frequency is most commonly obtained using discrete Fourier transformation (DFT) with the Doppler frequency in $_n$-th DFT bin given by $\omega_{D,n} = n \cdot \Delta\omega$, with $\Delta\omega$ being the frequency increment per DFT bin. Since $\Delta\omega$ is present in both $\Delta\Omega$ and $\omega_{D,i}$ it can be reduced and the calculations performed using DFT bin values.

Simultaneously with spectral calibration it is possible to find the unknown value of mirror mean velocity. From Fig. 1(b) we can find the Doppler frequency spread $\Delta\Omega$:

$$\Delta\Omega = \omega_{D,max} - \omega_{D,min} = 2vk_{max} - 2vk_{min} = 2vN_k\Delta k. \tag{14}$$

After combining Eq. (14) with Eq. (6) expression for mean velocity *v* can be given:

$$v = \Delta\Omega \cdot \frac{z_{max}}{\pi N_k}. \tag{15}$$

Biomedical Optics EXPRESS

3. Materials

3.1. SOCT setup

In the experiments we used supercontinuum light source (SuperK Power, NKT Photonics). The beam was split by the dichroic filter (Split, NKT Photonics) into visible and infrared channels. The light from the infrared channel (spectral range 690-1200 nm) was coupled to the fiber patchcord (Fiber Delivery FD3, NKT Photonics, spectral range 600-900 nm) and delivered to the experimental setup. The power at the input of the system was 16 mW.

The SOCT measurements were performed with use of the Michelson interferometer, see Fig. 2(a). The light from the light source was introduced to the fiber coupler of asymmetrical splitting ratio that transferred 70% of total light power to the interferometer. There the collimated beam was bifurcated by the beamsplitting cube into ARM 1 and ARM 2 arms. In ARM 1 dispersion compensation glass was placed to equalize the dispersion effects between ARM 1 and ARM 2. ARM 1 was terminated by the lens focusing the beam on the mirror fixed to the piezo-actuator (Physik Instrumente, Germany, 60 µm travel range). The actuator and the lens were mounted on the single-axis micrometer-precision translation stage (Thorlabs, USA) enabling setting up of optical path length difference between ARM 1 and ARM 2. In ARM 2 the beam passed through the variable neutral density filter, the focusing lens and was reflected back by the mirror.

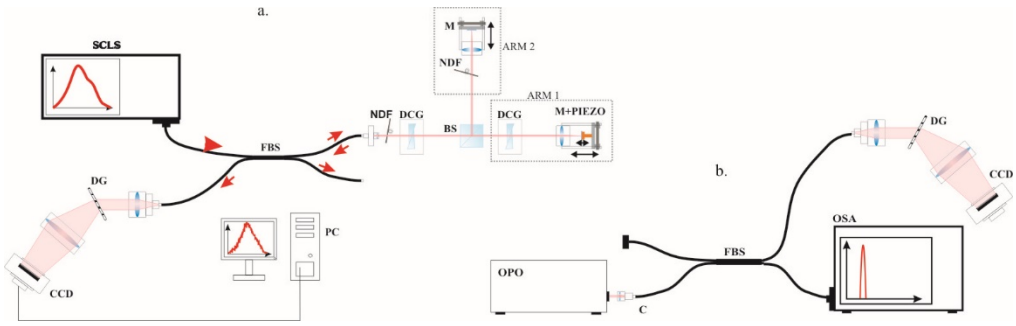

Fig. 2. a. Schematics of SOCT setup used in the experiments. SCLS – supercontinuum light source; FBS – fiber beam splitter; NDF – neutral density filter; DCG – dispersion compensation glass; BS – beam splitter; M – mirror; M + PIEZO – mirror mounted on a piezo-acutator; DG – diffraction grating; CCD – line CCD camera. b. Configuration used for reference procedure. OPO – optical parametric oscillator; OSA – optical spectrum analyzer.

Spectrometer used at detection side of the system was designed and optimized to work with the spectrum of the light as wide as 260 nm (spectral range: ~690 nm-950 nm). It was arranged in Littrow single-lens setup with high-performance collimator at the fiber output (Tele-Xenar 2.2/70 mm Schneider Kreuznach, Germany), 1200 lpmm highly efficient holographic diffraction grating with 830 nm antireflective coating (Wasatch Photonics, USA) and 100 mm focal length achromatic doublet (Thorlabs, USA). The light was detected by the single line camera (e2v, SM2 CL 2014, United Kingdom) with 2048 pixels and with 32 µs repetition time.

3.2. Validation procedure

The accuracy of the calibration method was verified with the use of the reference procedure involving well-defined spectral lines, see Fig. 2(b). To produce the marker lines we used tunable laser (fs-Emerald, APE, Germany, spectral range of the signal wavelength: 690-980 nm). The wavelength was tuned by means of adjustment of temperature of the crystal in optical parametric oscillator (OPO). The light from the source was coupled to the fiber patchcord and split by the fiber coupler (AC Photonics, USA, splitting ratio 50/50). One channel was connected directly to the spectrometer, second channel – to the optical spectrum

Biomedical Optics EXPRESS

analyzer (OSA, Yokogawa AQ6370B, Japan). The spectral resolution of the OSA is equal to 0.02 nm.

4. Results and discussion

In all the SOCT measurements mirrors were mounted in both arms of the interferometer. In order to show the calibration technique we have registered sets of data of four kinds acquired within 4 hours to minimize possible temporal drift of the spectrometer spectral range:

1. Data set 1. 60 images of the mirror moved by 20 μm along the whole in depth imaging range of the SOCT setup. The optical path difference was changed using a micrometer stage. At each position 1000 spectra were collected and averaged using complex averaging to increase signal-to-noise ratio (SNR) [38]. This data were used to linearize spectral fringes in wavenumber domain (Eq. (1) with q being phase difference as in Makita [20] and Wang [19] approaches), to calculate uncompensated dispersion and to find the imaging range $z_{\max}$.

2. Data set 2. 11 measurements acquired with one mirror mounted on a piezotransducer and moving with an unknown and nonlinear velocity. The nonlinearity of motion was caused by inertia of the mirror driven with saw tooth voltage. For each velocity 512 spectra were acquired during one-directional movement of the mirror. The velocities were chosen to be different in each measurement and to obey a rule not to exceed the maximal velocity measurable in the SOCT setup. Spectral fringes in these data sets were linearized in time domain (Eq. (1) with q being time-dependent phase for one wavelength), used to linearize spectral fringes in wavenumber domain (Eq. (1) with q being Doppler frequency as in Faber [21] approach) and to calculate wavenumber and wavelength for each point of the spectrum (Eqs. (13)-(14)).

3. Data sets 3&4. 13 OCT measurements of spectrally narrow lines from Optical Parametric Oscillator (OPO) covering spectral range from approximately 700 nm to 940 nm. The light was acquired simultaneously by SOCT spectrometer (Data set 3) and Optical Spectrum Analyzer (OSA, Data set 4). These data were used to verify the accuracy of spectral mapping.

The first step of spectrometer calibration is linearization of the spectra in wavenumber domain as described in Section 2.1. The above sets of data give two possible paths to linearize spectra to wavenumber domain which we compare below to find the more precise one.

In the first path (named Path 1 for simplicity), we obtain q values from images of mirror by following the Wang-Makita approach: we take five mirror images with highest signal-to-noise ratio (SNR) from Data set 1 and bandpass filter them to remove the DC signal along with the complex conjugate components. Next for each pair of the resulting complex spectral fringes we find the difference between phases which, after phase unwrapping, serve as q values for Eq. (1).

In the second path (named Path 2) we obtain q values from Doppler frequency in time dependent fringes from Data set 2 following a modified Faber approach. At first, each measurement is resampled in time to compensate for the nonlinear motion of the mirror as described in Section 2.2. This procedure is repeated for each measurement from Data set 2 separately. Next, to find the q values, the resampling in time procedure is followed by Fourier Transformation along time axis (what is equivalent to moving from kt plane to kw plane in the STdOCT diagram). As q values serve the positions (in DFT units) of the Doppler frequency.

In the second step the q values obtained by either Path 1 or Path 2 are used to calculate the resampling indexes using Eq. (1). The optimization procedure is used to find the optimal rank r of the polynomial as described in Section 2.1. As optimal rank r of the polynomial we have chosen the one that results in resampling indexes that minimize the resolution drop in the

Biomedical Optics EXPRESS

range from zero to approximately 1 mm of optical path difference (OPD). It has to be noted that in our setup the images of the mirror beyond approximately 1 mm are distorted due to the fact that parts of the spectral fringes from the side of higher wavenumbers cross the Nyquist limit. As a result, those images have only a part of the energy concentrated in the main lobe of the image and, consequently, lower amplitude and distorted width.

At this stage of the procedure we have 4 resampling indexes from Path 1 and 11 resampling indexes from Path 2. Figure 3(a) shows the difference between the mean of the resampling indexes and the resampling indexes calculated with different q values (Wang-Makita approach vs. Faber approach). It can be seen that after resolution drop optimization the resampling indexes obtained using different methods and different data sets are almost identical. The maximal difference between the mean indexes is approximately 1 pixel, while the standard deviation is smaller than 1.2 pixel for Wang-Makita approach (Path 1) and 2.6 pixel for Faber approach (Path 2).

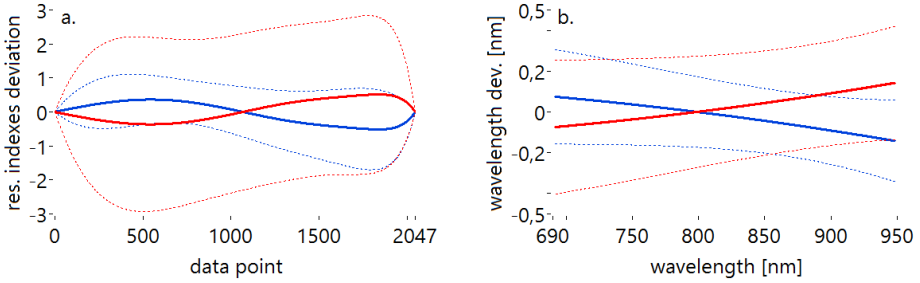

Fig. 3. a. Difference between mean resampling indexes and resampling indexes calculated using: (in red) Path 1 Wang-Makita approach, 4 different mirror position differences, and (blue) Path 2 Faber approach, 11 measurements with different Doppler frequencies. Solid lines are mean resampling indexes for each path while dotted lines are standard deviations. b Comparison of the wavelength calculated with resampling indexes from a. used to linearize Data set 2 and calculate imaging range.

To calculate the total imaging range we take advantage of the fact that the relative physical position of the mirror in Data set 1 is known from readings of the micrometer stage. Therefore, the imaging range of the SOCT setup can be calculated by fitting those positions to mirror position read from SOCT data. For proper reading of mirror positions from SOCT data the spectra from need to be resampled with optimized resampling Indexes and corrected for uncompensated dispersion. The imaging range obtained with resampling indexes from Path 1 is equal to 1306.80 ± 2.12 μm, while this obtained with resampling indexes from Path 2 is equal to 1308.90 ± 1.76 μm.

To map wavelengths to spectral points in both Paths we used measurements from Data set 2 already resampled in time as described earlier in this subsection. Next, the data from Data set 2 were resampled again to linearize them in wavenumber domain.

In Path 1 we first choose one measurement from Data set 2 and resample it to wavenumber domain with each of the 11 resampling indexes. In Path 2 for each measurement from Data set 2 we use the resampling indexes calculated from the same measurement. In both Paths, the imaging range is calculated from the Data set 1 resampled using the same resampling indexes as for resampling of Data set 2 measurements.

In both Paths when processing data chosen from Data set 2, after all linearizations, we Fourier transform the spectra along time axis to kω plane using FFT with zeropadding to 1024 points. Next, we find the positions of the peak frequency for each data pixel along the wavenumber axis. The position of the peak along frequency axis used in calculations is in units of FFT bins, no recalculations to any physical value is performed. Next, we fit the peak positions with a line according to the assumption from Eq. (4) and Eq. (11). At last, we insert

Biomedical Optics EXPRESS

as n_{Di} the values of the fitted line (calculated for all points along the wavenumber axis) to the Eq. (12) and Eq. (13) to obtain values of wavenumber and wavelength for all the points along the wavenumber axis. Figure 3(b) shows comparison of the wavelength calculations using both described paths. In Path 1 we have four different results with maximal standard deviation equal 0.33 nm. In Path 2 we have 11 results with maximal standard deviation equal 0.23 nm. The maximal difference between the mean values is equal 0.28 nm.

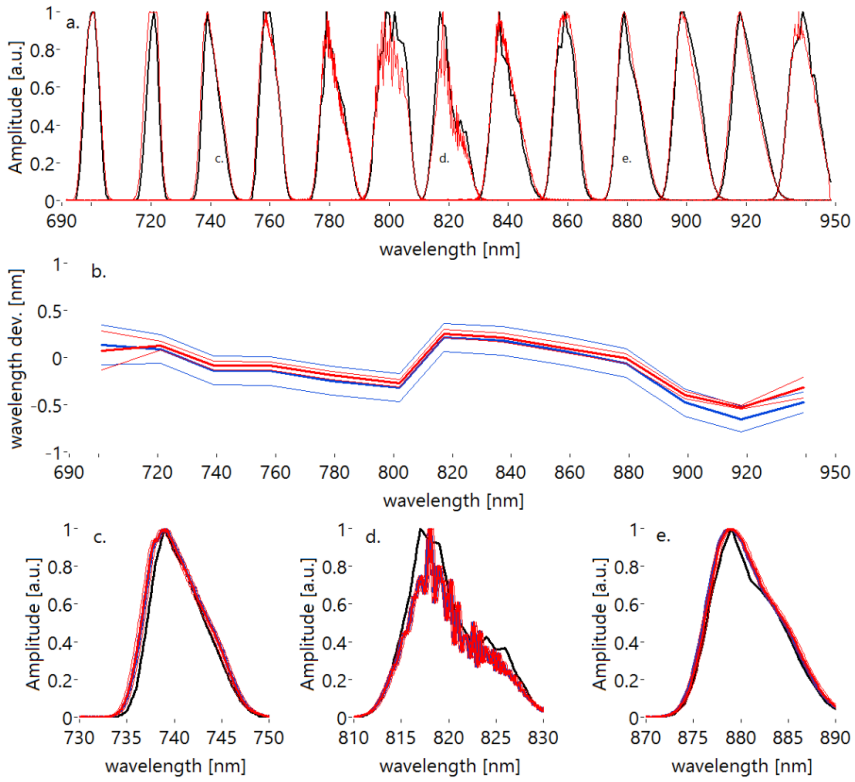

Fig. 4. a. Overlay of narrow spectral lines generated by optical parametric oscillator (OPO) and measured with (black) optical spectrum analyzer (OSA) and (red) SOCT spectrometer. The OCT data is plotted against wavelengths mean calculated following Path 1. b. Difference in wavelength position between spectral lines from generated with OPO measured with SOCT spectrometer. Wavelengths for SOCT data are calculated following (in red) Path 1 Wang-Makita approach, 4 different mirror position differences, and (in blue) Path 2 Faber approach, 11 measurements with different Doppler frequencies. c-e. OPO spectral lines from a. with overlaid wavelength errors from Fig. 3(b). Solid lines are spectral lines plotted against mean wavelength while dotted lines are standard deviations of wavelengths.

To validate obtained results we overlay spectrally narrow spectral lines obtained from Optical Parametric Oscillator (OPO) acquired simultaneously with Optical Spectrum Analyzer (OSA) and by the OCT spectrometer. All the lines have amplitude normalized to unity for sake of clarity. The OCT acquired data (Data set 3) are first resampled using the resampling indexes calculated by following Path 1 and Path 2 and are plotted in Fig. 4(a) as a function of wavelengths found using the same resampling indexes. Data from Data set 4 are overlaid on the same plot as a function of wavelength read from OSA. Figures 4(c)-4(e) show single lines in more detail along with wavelength error shown in Fig. 3(b).

In the next step we found the displacement in wavelengths of the lines imaged by OSA and SOCT spectrometers by means of cross correlation of the images. The result is plotted in Fig. 4(b). It can be seen that the difference of mean wavelengths obtained with the two Paths

Biomedical Optics EXPRESS

are almost identical: mean difference between centers of mass of spectral lines obtained from SOCT data and from OSA data is equal 0.12 nm for Path 1 and 0.13 nm for Path 2 with RMS equal to 0.25 nm for Path 1 and 0.30 nm for Path 2 This result suggests that the procedure with higher reliability is the one where the resampling indexes are calculated using the modified Wang-Makita approach extended with resampling indexes optimization along with dispersion calculation and compensation. Obtained accuracy of wavelength to pixel assignment is comparable to values 0.12-0.22 nm reported for calibration with other methods using Doppler frequency [21] or a set of spectrally narrow lines [32]. The advantage of our method is that it does not require neither precise knowledge about mirror velocity nor any additional light source. Moreover, an important advantage is the resistance of the method to nonlinear velocity of the sample mirror. As a result, the spectral calibration may be easily performed with good accuracy with any device that can continuously displace the mirror in the sample arm.

5. Conclusions

We proposed and tested a robust technique of wavelength mapping of the SOCT spectra that uses solely data acquired by the spectrometer to be calibrated. The procedure can in principle use any physical quantity that is linear in wavenumbers and can be measured using the spectrometer to be calibrated. The actual value of the physical quantity used for calibration is not necessarily to be known at any stage of the procedure and can be set with little care, what increases the robustness of the technique.

The presented wavelength mapping technique requires spectral fringes acquired by the spectrometer to be linear in wavenumber domain. This requirement can be fulfilled in the spectrometers by numerical postprocessing. For the purpose of comprehensiveness of the approach we show an optimization procedure that minimizes resolution drop as a function of depth and removes effects of nonlinear sampling and uncompensated dispersion on the SOCT spectra. The wavelength mapping method requires only one additional physical parameter of the SOCT setup that has to be measured: the depth imaging range. This is the strong advantage of the proposed approach since the depth imaging range is one of the SOCT setup properties that can be assessed with ease using simple calibrated mechanical stages.

Both steps of the procedure, namely linearization of spectra to wavenumber domain with dispersion compensation and wavenumber to pixel mapping, may use any (the same or different) physical quantity with values linear in wavenumber domain that can be detected by the spectrometer to be calibrated. In this work we showed that the Doppler frequency induced by a mirror moving in the sample arm of SOCT spectrometer can serve as calibration quantity. The motion of the mirror can be nonlinear as application of a simple resampling technique allows to extract the mean Doppler frequency with sufficient precision. The whole calibration of the spectrometer including wavenumber linearization and wavelength calibration can be performed using only two SOCT sets of measurements: one obtained with the sample arm mirror positioned over all imaging range (to calculate the imaging range and to be used in the procedure to optimize the resolution drop) and the second one with the sample arm mirror moving with linear or nonlinear velocity. We show that using such data, two different paths of calculation yield almost identical wavelength to pixel mappings.

In principle the technique can be applied to any FdOCT setup including Swept Source OCT devices.

Funding

Polish National Center for Research and Development (NCBR) (PBS1/A9/20/2013); Polish Ministry of Science and Higher Education (“Iuventus Plus” programme for years 2015-2016 grant IP 2014 045973).